Chapter 3
Analysis of the Interferometer Response

In this chapter, we introduce the full two-dimensional analysis of the interferometer response, without small-angle assumptions, and then investigate the small-field approximations that simplify the transformation from the measured visibility to the intensity distribution. There is a discussion of the relationship between the cross-correlation of the received signals and the cross power spectrum, which results from the Wiener–Khinchin relation and is fundamental to spectral line interferometry. An analysis of the basic response of the receiving system is also given. The appendix considers some approaches to the representation of noiselike signals, including the analytic signal, and truncation of the range of integration.

3.1 Fourier Transform Relationship Between Intensity and Visibility

3.1.1 General Case

We begin by deriving the relationship between intensity and visibility in a coordinate-free form and then show how the choice of a coordinate system results in an expression in the familiar form of the Fourier transform. Suppose that the antennas track the source under observation, which is the most common situation, and let the unit vector $\mathbf{s}_0$ in Fig. 3.1 indicate the phase reference position introduced in Sect. 2.3. This position, sometimes also known as the phase-tracking center, becomes the center of the field to be imaged. For one polarization, an element of the source of solid angle $d\Omega$ at position $\mathbf{s} = \mathbf{s}_0 + \boldsymbol{\sigma}$ contributes a component of power $\frac{1}{2}A(\boldsymbol{\sigma})I(\boldsymbol{\sigma})\Delta\nu d\Omega$ at each of the two antennas. Here, $A(\boldsymbol{\sigma})$ is the effective collecting area of each antenna, $I(\boldsymbol{\sigma})$ is the source intensity distribution as observed

A.R. Thompson, J.M. Moran, and G.W. Swenson Jr., *Interferometry and Synthesis in Radio Astronomy*, Astronomy and Astrophysics Library,
DOI 10.1007/978-3-319-44431-4_3

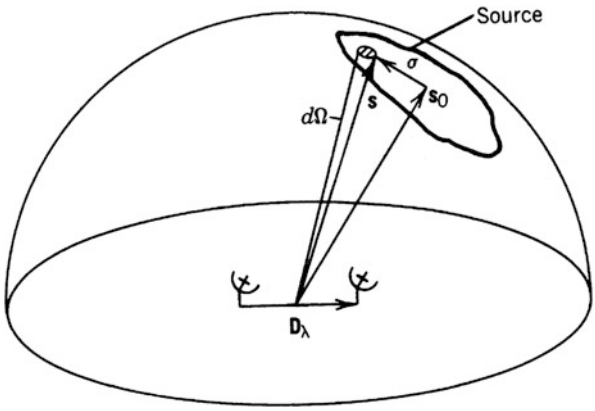

Fig. 3.1 Baseline and position vectors that specify the interferometer and the source. The source is represented by the outline on the celestial sphere.

from the distance of the antennas, and $\Delta\nu$ is the bandwidth of the receiving system. It is easily seen that this expression has the dimensions of power since the units of I are W m^{-2} Hz^{-1} sr^{-1}. From the considerations outlined in the derivation of Eqs. (2.1) and (2.2), including the far-field condition for the source, the resulting component of the correlator output is proportional to the received power and to the fringe term $\cos(2\pi\nu\tau_g)$, where τ_g is the geometric delay. The vector $\mathbf{D}_\lambda$ will specify the baseline measured in wavelengths, and then $\nu\tau_g = \mathbf{D}_\lambda \cdot \mathbf{s} = \mathbf{D}_\lambda \cdot (\mathbf{s}_0 + \boldsymbol{\sigma})$. Thus, the output from the correlator is represented by

$$\begin{aligned} r(\mathbf{D}_\lambda, \mathbf{s}_0) &= \Delta\nu \int_{4\pi} A(\boldsymbol{\sigma}) I(\boldsymbol{\sigma}) \cos\left[2\pi\ \mathbf{D}_\lambda \cdot (\mathbf{s}_0 + \boldsymbol{\sigma})\right] d\Omega \\ &= \Delta\nu \cos(2\pi \mathbf{D}_\lambda \cdot \mathbf{s}_0) \int_{4\pi} A(\boldsymbol{\sigma}) I(\boldsymbol{\sigma}) \cos(2\pi \mathbf{D}_\lambda \cdot \boldsymbol{\sigma})\, d\Omega \\ &\quad - \Delta\nu \sin(2\pi \mathbf{D}_\lambda \cdot \mathbf{s}_0) \int_{4\pi} A(\boldsymbol{\sigma}) I(\boldsymbol{\sigma}) \sin(2\pi \mathbf{D}_\lambda \cdot \boldsymbol{\sigma})\, d\Omega\ . \end{aligned} \tag{3.1}$$

Note that the integration of the response to the element $d\Omega$ over the source in Eq. (3.1) requires the assumption that the source is spatially incoherent, that is, that the radiated waveforms from different elements $d\Omega$ are uncorrelated. This assumption is justified for essentially all cosmic radio sources. Spatial coherence is discussed further in Sect. 15.2. Let A_0 be the antenna collecting area in direction $\mathbf{s}_0$ in which the beam is pointed. We introduce a normalized reception pattern $A_N(\boldsymbol{\sigma}) = A(\boldsymbol{\sigma})/A_0$ and consider the modified intensity distribution $A_N(\boldsymbol{\sigma})I(\boldsymbol{\sigma})$. Now

we define the complex visibility[1] as

$$\mathcal{V} = |\mathcal{V}|e^{j\phi_v} = \int_{4\pi} A_N(\boldsymbol{\sigma}) I(\boldsymbol{\sigma})\, e^{-j2\pi \mathbf{D}_\lambda \cdot \boldsymbol{\sigma}} d\Omega \ . \tag{3.2}$$

Then by separating the real and imaginary parts, we obtain

$$\int_{4\pi} A_N(\boldsymbol{\sigma}) I(\boldsymbol{\sigma})\ \cos(2\pi \mathbf{D}_\lambda \cdot \boldsymbol{\sigma})\, d\Omega = |\mathcal{V}| \cos\phi_v \ , \tag{3.3}$$

$$\int_{4\pi} A_N(\boldsymbol{\sigma}) I(\boldsymbol{\sigma})\ \sin(2\pi \mathbf{D}_\lambda \cdot \boldsymbol{\sigma})\, d\Omega = -|\mathcal{V}| \sin\phi_v \ , \tag{3.4}$$

and from Eq. (3.1)

$$r(\mathbf{D}_\lambda, \mathbf{s}_0) = A_0 \Delta\nu |\mathcal{V}| \cos(2\pi \mathbf{D}_\lambda \cdot \mathbf{s}_0 - \phi_v) \ . \tag{3.5}$$

Thus, the output of the correlator can be expressed in terms of a fringe pattern corresponding to that for a hypothetical point source in the direction $\mathbf{s}_0$, which is the phase reference position. As noted earlier, this is usually the center or nominal position of the source to be imaged. The modulus and phase of $\mathcal{V}$ are equal to the amplitude and phase of the fringes; the phase is measured relative to the fringe phase for the hypothetical source. As defined above, $\mathcal{V}$ has the dimensions of flux density (W m^{-2} Hz^{-1}), which is consistent with its Fourier transform relationship with I. Some authors have defined visibility as a normalized, dimensionless quantity, in which case it is necessary to reintroduce the intensity scale in the resulting image. Note that the bandwidth has been assumed to be small compared with the center frequency in deriving Eq. (3.5).

In introducing a coordinate system, the geometry we now consider is illustrated in Fig. 3.2. The two antennas track the center of the field to be imaged. They are assumed to be identical, but if they differ, $A_N(\boldsymbol{\sigma})$ is the geometric mean of the beam patterns of the two antennas. The magnitude of the baseline vector is measured in wavelengths at the center frequency of the observing band, and the baseline has components (u, v, w) in a right-handed coordinate system, where u and v are measured in a plane normal to the direction of the phase reference position. The spacing component v is measured toward the north as defined by the plane through the origin, the source, and the pole, and u is measured toward the east.

[1] In formulating the fundamental Fourier transform relationship in synthesis imaging, which follows from Eq. (3.2), we use the negative exponent to derive the complex visibility function (or mutual coherence function) from the intensity distribution, and the positive exponent for the inverse operation. From a physical viewpoint, the choice is purely arbitrary, and the literature contains examples of both this and the reverse convention. Our choice follows Born and Wolf (1999) and Bracewell (1958).

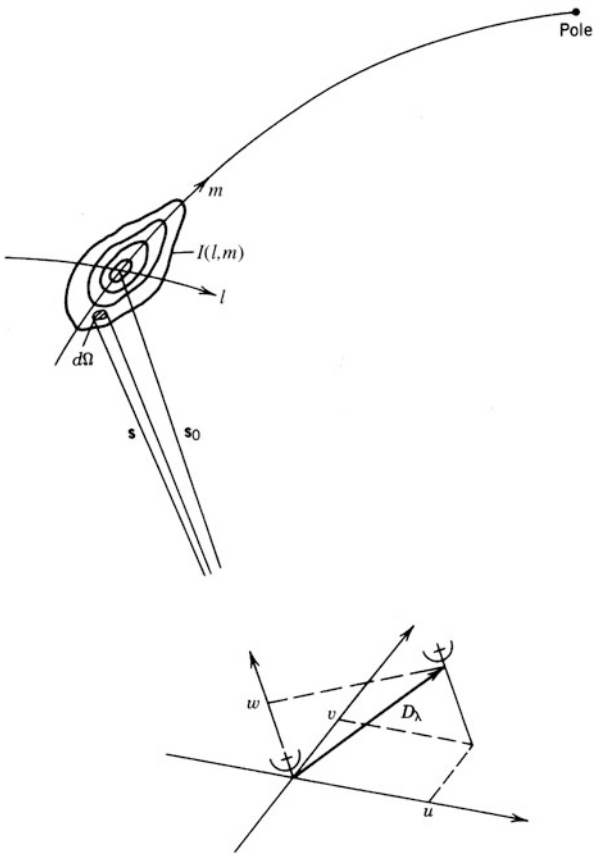

Fig. 3.2 Geometric relationship between a source under observation $I(l, m)$ and an interferometer or one antenna pair of an array. The antenna baseline vector, measured in wavelengths, has length D_λ and components (u, v, w).

The component w is measured in the direction $\mathbf{s}_0$, which is the phase reference position. On Fourier transformation, the phase reference position becomes the origin of the derived intensity distribution $I(l, m)$, where l and m are direction cosines measured with respect to the axes u and v. In terms of these coordinates, we find

$$\begin{aligned}
\mathbf{D}_\lambda \cdot \mathbf{s}_0 &= w \\
\mathbf{D}_\lambda \cdot \mathbf{s} &= \left(ul + vm + w\sqrt{1 - l^2 - m^2} \right) \\
d\Omega &= \frac{dl\, dm}{\sqrt{1 - l^2 - m^2}} \,,
\end{aligned} \tag{3.6}$$

where $\sqrt{1-l^2-m^2}$ is equal to the third direction cosine n measured with respect to the w axis.[2] Note also that $\mathbf{D}_\lambda \cdot \boldsymbol{\sigma} = \mathbf{D}_\lambda \cdot \mathbf{s} - \mathbf{D}_\lambda \cdot \mathbf{s}_0$. Thus, from Eq. (3.2):

$$\mathcal{V}(u,v,w) = \int_{-\infty}^{\infty}\int_{-\infty}^{\infty} A_N(l,m)I(l,m) \times \exp\left\{-j2\pi\left[ul+vm+w\left(\sqrt{1-l^2-m^2}-1\right)\right]\right\}\frac{dl\,dm}{\sqrt{1-l^2-m^2}}\,. \tag{3.7}$$

A factor $e^{j2\pi w}$ on the right side in Eq. (3.7) results from the measurement of angular position with respect to the w axis. For a source on the w axis, $l = m = 0$, and the argument of the exponential term in Eq. (3.7) is zero. For any other source, the fringe phase is measured relative to that for a source on the w axis, which is the phase reference position, $\mathbf{s}_0$ in Fig. 3.2. The function $A_N I$ in Eq. (3.7) is zero for $l^2+m^2 \geq 1$, and in practice, it usually falls to very low values for directions outside the field to be imaged, as a result of the antenna beam pattern, the bandwidth pattern, or the finite size of the source. Thus, we can extend the limits of integration to $\pm\infty$. Note, however, that Eq. (3.7) requires no small-angle assumptions. The reason why we use direction cosines rather than a linear measure of angle in interferometer theory is that they occur in the exponential term of this relationship.

The coordinate system (l,m) defined above is a convenient one in which to present an intensity distribution. It corresponds to the projection of the celestial sphere onto a plane that is a tangent at the field center, as shown in Fig. 3.3. The distance of any point in the image from the (l,m) origin is proportional to the sine of the corresponding angle on the sky, so for small fields, distances on the image are closely proportional to the corresponding angles. The same relationship usually applies to the field of an optical telescope. For a detailed discussion of relationships on the celestial sphere and tangent planes, see König (1962).

If all the measurements could be made with the antennas in a plane normal to the w direction so that $w = 0$, Eq. (3.7) would reduce to an exact two-dimensional Fourier transform. In general, this is not possible, and we now consider ways in which the transform relationship can be applied. Recall first that the basis of the

[2]The expression for $d\Omega$ is obtained by considering the unit sphere centered on the (u,v,w) origin. A point P on the sphere with coordinates (u,v,w) is projected onto the (u,v) plane at $u = l, v = m$, and the increments dl, dm define a column of square cross section running through $(u,v,0)$ parallel to the w axis. The column makes an angle $\cos^{-1} n$ with the normal to the spherical surface at P, and $d\Omega$ is equal to the surface area intersected by the column, which is $dl\,dm/n$, or $dl\,dm/\sqrt{1-l^2-m^2}$. Alternately, the solid angle can be expressed in polar coordinates as $d\Omega = \sin\theta\, d\theta\, d\phi$, where θ and ϕ are the polar and azimuthal angles in the (u,v,w) plane, that is, $\theta = \sin^{-1}\sqrt{l^2+m^2}$ and $\phi = \tan^{-1} m/l$. Calculation of the Jacobian of the transformation from (θ,ϕ) coordinates to (l,m) coordinates gives the result $d\Omega = dl\,dm/\sqrt{1-l^2-m^2}$ (Apostol 1962).

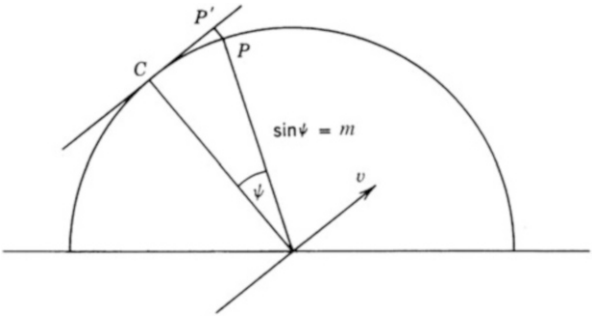

Fig. 3.3 Mapping of the celestial sphere onto an image plane, shown in one dimension. The position of the point P is measured in terms of the direction cosine m with respect to the v axis. When projected onto a plane surface with a scale linear in m, P appears at P' at a distance from the field center C proportional to $\sin\psi$.

synthesis imaging process is the measurement of $\mathcal{V}$ over a wide range of u and v. For a ground-based array, this can be achieved by varying the length and direction of the antenna spacing and also by tracking the field-center position as the Earth rotates. The rotation causes the projection of $\mathbf{D}_\lambda$ to move across the (u, v) plane, and an observation may last for 6–12 h. As the Earth's rotation carries the antennas through space, the baseline vector remains in a plane only if $\mathbf{D}_\lambda$ has no component parallel to the rotation axis, that is, the baseline is an east–west line on the Earth's surface. In the general case, there is a three-dimensional distribution of the measurements of $\mathcal{V}$. The simplest form of the transform relationship that can then be used is based on an approximation that is valid so long as the synthesized field is not too large. If l and m are small enough that the term

$$\left(\sqrt{(1-l^2-m^2)}-1\right)w \simeq -\tfrac{1}{2}(l^2+m^2)w \tag{3.8}$$

can be neglected, Eq. (3.7) becomes

$$\mathcal{V}(u,v,w) \simeq \mathcal{V}(u,v,0) = \int_{-\infty}^{\infty}\int_{-\infty}^{\infty} \frac{A_N(l,m)I(l,m)}{\sqrt{1-l^2-m^2}} e^{-j2\pi(ul+vm)}\, dl\, dm\ . \tag{3.9}$$

Thus, for a restricted range of l and m, $\mathcal{V}(u,v,w)$ is approximately independent of w, and for the inverse transform, we can write

$$\frac{A_N(l,m)I(l,m)}{\sqrt{1-l^2-m^2}} = \int_{-\infty}^{\infty}\int_{-\infty}^{\infty} \mathcal{V}(u,v)\, e^{j2\pi(ul+vm)}\, du\, dv\ . \tag{3.10}$$

With this approximation, it is usual to omit the w dependence and write the visibility as the two-dimensional function $\mathcal{V}(u,v)$. Note that the factor $\sqrt{1-l^2-m^2}$ in Eqs. (3.9) and (3.10) can be subsumed into the function $A_N(l,m)$. Equation (3.10) is a form of the van Cittert–Zernike theorem, which originated in optics and is discussed in Sect. 15.1.1.

The approximation in Eq. (3.9) introduces a phase error equal to 2π times the neglected term, that is, $\pi(l^2+m^2)w$. Limitation of this error to some tolerable value places a restriction on the size of the synthesized field, which can be estimated

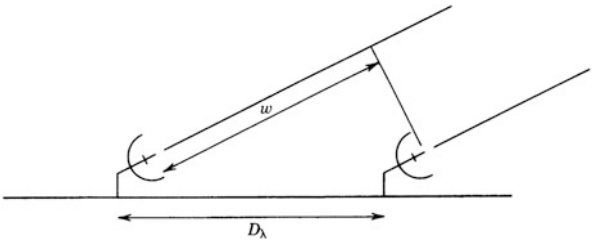

Fig. 3.4 When observations are made at a low angle of elevation and at an azimuth close to that of the baseline, the spacing component w becomes comparable to the baseline length D_λ, which is measured in wavelengths.

approximately as follows. If the antennas track the source under observation down to low elevation angles, the values of w can approach the maximum spacings $(D_\lambda)_{\max}$ in the array, as shown in Fig. 3.4. Also, if the spatial frequencies measured are evenly distributed out to the maximum spacing, the synthesized beamwidth θ_b is approximately equal to $(D_\lambda)^{-1}_{\max}$. Thus, the maximum phase error is approximately

$$\pi \left(\frac{\theta_f}{2}\right)^2 \theta_b^{-1} , \tag{3.11}$$

where θ_f is the width of the synthesized field. The condition that no phase errors can exceed, say, 0.1 rad then requires that

$$\theta_f < \tfrac{1}{3}\sqrt{\theta_b} , \tag{3.12}$$

where the angles are measured in radians. For example, if $\theta_b = 1''$, $\theta_f < 2.5$ arcmin. Much synthesis imaging in astronomy is performed within this restriction, and ways of imaging larger fields will be discussed later.

3.1.2 East–West Linear Arrays

We now turn to the case of arrays with east–west spacings only and discuss further the conditions for which we can put $w = 0$, and the resulting effects. Let us first rotate the (u, v, w) coordinate system about the u axis until the w axis points toward the pole, as shown in Fig. 3.5. We indicate by primes the quantities measured in the rotated system. The (u', v') axes lie in a plane parallel to the Earth's equator. The east–west antenna spacings contain components in this plane only (i.e., $w' = 0$), and as the Earth rotates, the spacing vectors sweep out circles concentric with the (u', v') origin. From Eq. (3.7), we can write

$$\mathcal{V}(u', v') = \int_{-\infty}^{\infty}\int_{-\infty}^{\infty} A_N(l', m') I(l', m')\, e^{-j2\pi(u'l' + v'm')} \frac{dl'\,dm'}{\sqrt{1 - l'^2 - m'^2}} , \tag{3.13}$$

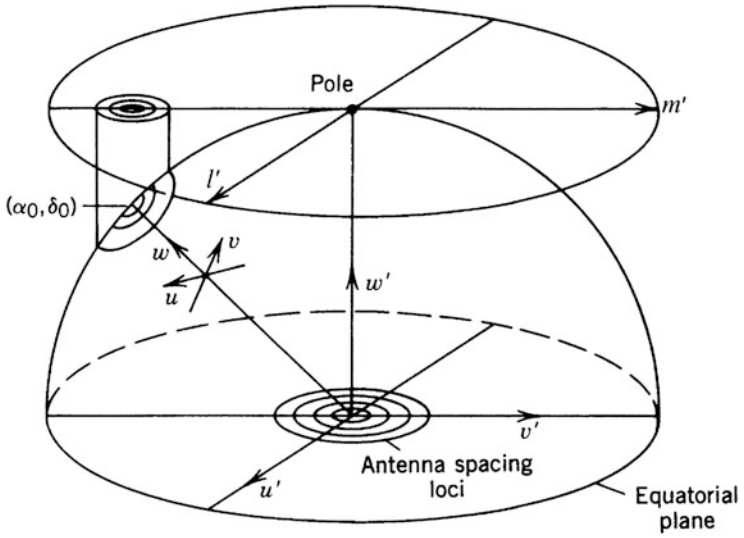

Fig. 3.5 The (u', v', w') coordinate system for an east–west array. The (u', v') plane is the equatorial plane and the antenna spacing vectors trace out arcs of concentric circles as the Earth rotates. Note that the directions of the u' and v' axes are chosen so that the v' axis lies in the plane containing the pole, the observer, and the point under observation (α_0, δ_0). In Fourier transformation from the (u', v') to the (l', m') planes, the celestial hemisphere is imaged as a projection onto the tangent plane at the pole. The (u, v, w) coordinates for observation in the direction (α_0, δ_0) are also shown.

where (l', m') are direction cosines measured with respect to (u', v'). Equation (3.13) holds for the whole hemisphere above the equatorial plane. The inverse transformation yields

$$\frac{A_N(l', m')I(l', m')}{\sqrt{1 - l'^2 - m'^2}} = \int_{-\infty}^{\infty}\int_{-\infty}^{\infty} \mathcal{V}(u', v')\, e^{j2\pi(u'l' + v'm')} du' dv' \ . \tag{3.14}$$

In this imaging, the hemisphere is projected onto the tangent plane at the pole, as shown in Fig. 3.5. In practice, however, an image may be confined to a small area within the antenna beams. In the vicinity of such an area, centered at right ascension and declination (α_0, δ_0), angular distances in the image are compressed by a factor $\sin \delta_0$ in the m' dimension. Also, in imaging the (α_0, δ_0) vicinity, it is convenient if the origin of the angular position variables is shifted to (α_0, δ_0). Expansion of the scale and shift of the origin can be accomplished by the coordinate transformation

$$l = l', \qquad m'' = (m' - \cos \delta_0) \operatorname{cosec} \delta_0 \ . \tag{3.15}$$

If we write $F(l', m')$ for the left side of Eq. (3.14), then

$$F(l', m') \longleftrightarrow \mathcal{V}(u', v') \ , \tag{3.16}$$

and

$$F\left[l', (m' - \cos\delta_0)\operatorname{cosec}\delta_0\right] \longleftrightarrow |\sin\delta_0|\,\mathcal{V}(u', v'\sin\delta_0)e^{-j2\pi v'\cos\delta_0} \ , \tag{3.17}$$

where $\longleftrightarrow$ indicates Fourier transformation. Equation (3.17) follows from the behavior of Fourier pairs with change of variable and involves the shift and similarity properties of Fourier transforms (see Appendix 2.1). The coordinates $(u', v'\sin\delta_0)$ on the right side of Eq. (3.17) represent the projection of the equatorial plane onto the (u, v) plane, which is normal to the direction (α_0, δ_0). In the (u, v, w) system, $u = u'$ and $v = v'\sin\delta_0$. The coordinate w shown in Fig. 3.5 is equal to $-v'\cos\delta_0$. Thus, $e^{-j2\pi v'\cos\delta_0}$ in Eq. (3.17) is the same factor that occurs in Eq. (3.7) as a result of the measurement of visibility phase relative to that for a point source in the w direction. Equation (3.14) now becomes

$$\begin{aligned}\frac{A_N(l, m'')I(l, m'')}{\sqrt{1 - l^2 - m''^2}} &= \int_{-\infty}^{\infty}\int_{-\infty}^{\infty} \mathcal{V}(u', v'\sin\delta_0)\,|\sin\delta_0|\,e^{-j2\pi v'\cos\delta_0} \\ &\quad \times e^{j2\pi(u'l' + v'm')}du'dv' \\ &= \int_{-\infty}^{\infty}\int_{-\infty}^{\infty} \mathcal{V}(u, v)\,e^{j2\pi(ul + vm'')}du\,dv \ . \end{aligned} \tag{3.18}$$

A similar analysis is given by Brouw (1971).

The derivation of Eq. (3.18) from Eq. (3.14) involves a redefinition of the m coordinate but no approximations. Equation (3.18) is of the same form as Eq. (3.10), in which the term in Eq. (3.8) was neglected. Thus, if we apply the imaging scheme of Eq. (3.10), which is based on omitting this term, to observations made with an east–west array, the phase errors introduced distort the image in a way that corresponds exactly to the change of definition of the m variable to m''. Since m'' is derived from a direction cosine measured from the v' axis in the equatorial plane, there is a progressive change in the north–south angular scale over the image. The factor cosec δ_0 in Eq. (3.15) establishes the correct angular scale at the center of the image, but this simple correction is acceptable only for small fields. The crucial point to note here is that when visibility data measured in a plane are projected into (u, v, w) coordinates, w is a linear function of u and v (and a linear function of v alone for east–west baselines). Hence, the phase error $\pi(l^2 + m^2)w$ is linear in u and v. Phase errors of this kind have the effect of introducing position shifts in the resulting image, but there remains a one-to-one correspondence between points in the image and on the sky. The effect is simply to produce a predictable, and hence correctable, distortion of the coordinates.

It is clear from Fig. 3.5 that if all the measurements lie in the (u', v') plane, then the values of v in the (u, v) plane become seriously foreshortened for directions close to the celestial equator. Obtaining two-dimensional resolution in such directions requires components of antenna spacing parallel to the Earth's axis. The design of such arrays is discussed in Chap. 5. The effect of the Earth's rotation is then to distribute the measurements in (u, v, w) space so that they no longer lie in a plane, unless the observation is of short time duration. In some cases, the restriction of the synthesized field in Eq. (3.12) is acceptable. In other cases, it may be necessary to image the entire beam to avoid source confusion, and several techniques are possible based on the following approaches:

1. Equation (3.7) can be written in the form of a three-dimensional Fourier transform. The resulting intensity distribution is then taken from the surface of a unit sphere in (l, m, n) space.
2. Large images can be constructed as mosaics of smaller ones that individually comply with the field restriction for two-dimensional transformation. The centers of the individual images must be taken at tangent points on the same unit sphere referred to in 1.
3. Since in most terrestrial arrays the antennas are mounted on an approximately plane area of ground, measurements taken over a short time interval lie close to a plane in (u, v, w) space. It is therefore possible to analyze an observation lasting several hours as a series of short duration images, which are subsequently combined after adjustment of the coordinate scales.

Practical implementation of the three approaches outlined above requires the nonlinear deconvolution techniques described in Chap. 11. A more detailed discussion of the resulting methods is given in Sect. 11.7.

3.2 Cross-Correlation and the Wiener–Khinchin Relation

The Fourier transform relationship between the power spectrum of a waveform and its autocorrelation function, the Wiener–Khinchin relation, is expressed in Eqs. (2.6) and (2.7). It is also useful to examine the corresponding relation for the cross-correlation function of two different waveforms. The response of a correlator, as used in a radio interferometer, can be written as

$$r(\tau) = \lim_{T\to\infty} \frac{1}{2T} \int_{-T}^{T} V_1(t) V_2^*(t-\tau)\, dt\ , \tag{3.19}$$

where the superscript asterisk indicates the complex conjugate. In practice, the correlation is measured for a finite time period $2T$, which is usually a few seconds or minutes but is long compared with both the period and the reciprocal bandwidth of the waveforms. The factor $1/2T$ is sometimes omitted, but for the waveforms considered here, it is required to obtain convergence. Cross-correlation

is represented by the pentagram symbol ($\star$):

$$V_1(t) \star V_2(t) = \lim_{T\to\infty} \frac{1}{2T} \int_{-T}^{T} V_1(t) V_2^*(t-\tau)\, dt \ . \tag{3.20}$$

This integral can be expressed as a convolution in the following way:

$$V_1(t) \star V_2(t) = \lim_{T\to\infty} \frac{1}{2T} \int_{-\infty}^{\infty} V_1(t) V_{2-}^*(\tau - t)\, dt = V_1(t) * V_{2-}^*(t) \ , \tag{3.21}$$

where $V_{2-}(t) = V_2(-t)$. Now the ν, t Fourier transforms are as follows[3]: $V_1(t) \longleftrightarrow \widehat{V}_1(\nu)$, $V_2(t) \longleftrightarrow \widehat{V}_2(\nu)$, and $V_{2-}^*(t) \longleftrightarrow \widehat{V}_2^*(\nu)$. Then from the convolution theorem,

$$V_1(t) \star V_2(t) \longleftrightarrow \widehat{V}_1(\nu) \widehat{V}_2^*(\nu) \ . \tag{3.22}$$

The right side of Eq. (3.22) is known as the cross power spectrum of $V_1(t)$ and $V_2(t)$. The cross power spectrum is a function of frequency, and we see that it is the Fourier transform of the cross-correlation, which is a function of τ. This is a useful result, and in the case where $V_1 = V_2$, it becomes the Wiener–Khinchin relation. The relationship expressed in Eq. (3.22) is the basis of cross-correlation spectrometry, described in Sect. 8.8.2.

3.3 Basic Response of the Receiving System

From a mathematical viewpoint, the basic components of the interferometer receiving system are the antennas that transform the incident electric fields into voltage waveforms, the filters that select the frequency components to be processed, and the correlator that forms the averaged product of the signals. In the filter and the correlator, the signals may be in either analog or digital form. These components are shown in Fig. 3.6. Most other effects can be represented by multiplicative gain constants, which we shall ignore here, or as variations of the frequency response that can be subsumed into the expressions for the filters. Thus, we assume that the frequency response of the antennas and the strength of the received signal are effectively constant over the filter passband, which is realistic for many continuum observations.

[3] In this chapter, in cases where the same letter is used for functions of both time and frequency, the circumflex (hat) accent is used to indicate functions of frequency.

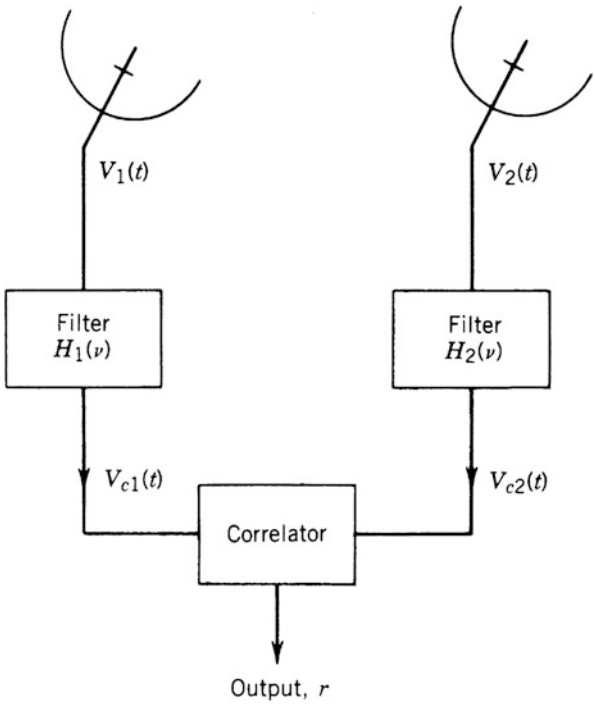

Fig. 3.6 Basic components of the receiving system of a two-element interferometer.

3.3.1 Antennas

In order to consider the responses of the two antennas independently, we should introduce their voltage reception patterns, since the correlator responds to the product of the signal voltages. The voltage reception pattern of an antenna $V_A(l, m)$ has the dimension *length* and responds to the electric field specified in volts per meter. $V_A(l, m)$ is the Fourier transform of the field distribution in the aperture $\overline{\mathcal{E}}(X, Y)$, as shown in Sect. 15.1.2. X and Y are coordinates of position within the antenna aperture. Omitting constant factors, we can write

$$V_A(l, m) \propto \int \int_{-\infty}^{\infty} \overline{\mathcal{E}}(X, Y)\, e^{j2\pi[(X/\lambda)l+(Y/\lambda)m]} dX\, dY\ , \tag{3.23}$$

where λ is the wavelength. In applying Eq. (3.23), X and Y are measured from the center of each antenna aperture. The power reception pattern is proportional to the squared modulus of the voltage reception pattern. $V_A(l, m)$ is a complex quantity, and it represents the phase of the radio frequency voltage at the antenna terminals as well as the amplitude. For an interferometer (with antennas denoted by subscripts 1 and 2), the response is proportional to $V_{A1} V_{A2}^*$, which is purely real if the antennas are identical. For each antenna, the collecting area $A(l, m)$ is a real quantity. In practice, it is usual to specify the antenna response in terms of $A(l, m)$ and to replace

$V_A(l,m)$ by $\sqrt{A(l,m)}$, which is proportional to the modulus of $V_A(l,m)$. Any phase introduced by differences between the antennas is ignored in this analysis but in effect is combined with the phase responses of the amplifiers, filters, transmission lines, and other elements that make up the signal path to the correlator input. The overall instrumental response of the interferometer in both phase and amplitude is calibrated by observing an unresolved source of known position and flux density.

For the case in which the antennas track the source, both the antenna beam center and the center of the source are at the (l,m) origin. If $E(l,m)$ is the incident field, the output voltage of an antenna can be written (omitting constant gain factors) as

$$\widehat{V} = \int\int_{-\infty}^{\infty} E(l,m)\sqrt{A(l,m)}\,dl\,dm\ . \tag{3.24}$$

If the antennas do not track the source, a convolution relationship of the form shown in Eq. (2.15) applies.

3.3.2 Filters

The filters in Fig. 3.6 will be regarded as a representation of the overall effect of components that determine the frequency response of the receiving channels, including amplifiers, cables, filters, and other components. The frequency response of a filter will be represented by $H(\nu)$, which can also be called the bandpass function. The output of the filter $\widehat{V}_c(\nu)$ is related to the input $\widehat{V}(\nu)$ by

$$\widehat{V}_c(\nu) = H(\nu)\widehat{V}(\nu)\ . \tag{3.25}$$

The Fourier transform of $H(\nu)$ with respect to time and frequency is the impulse response of the filter $h(t)$, which is the response to a voltage impulse $\delta(t)$ at the input. Thus, in the time domain, the corresponding expression to Eq. (3.25) is

$$V_c(t) = \int_{-\infty}^{\infty} h(t')V(t-t')\,dt' = h(t) * V(t)\ , \tag{3.26}$$

where the centerline asterisk represents convolution. In specifying filters, it is usual to use the frequency response rather than the impulse response because the former is more directly related to the properties of interest in a receiving system and is usually easier to measure.

3.3.3 Correlator

The correlator[4] produces the cross-correlation of the two voltages fed to it. If $V_1(t)$ and $V_2(t)$ are the input voltages, the correlator output is

$$r(\tau) = \lim_{T\to\infty} \frac{1}{2T} \int_{-T}^{T} V_1(t) V_2^*(t-\tau)\, dt\ , \tag{3.27}$$

where τ is the time by which voltage V_2 is delayed with respect to voltage V_1. For continuum observations, τ is maintained small or zero. The functions V_1 and V_2 that represent the signals may be complex. The output of a single multiplying device is a real voltage or number. To obtain the complex cross-correlation, which represents both the amplitude and the phase of the visibility, one can record the fringe oscillations and measure their phase, or use a *complex correlator* that contains two multiplying circuits, as described in Sect. 6.1.7. As follows from Eqs. (3.20) and (3.22), the Fourier transform of $r(\tau)$ is the cross power spectrum, which is required in observations of spectral lines. This can be obtained by inserting a series of instrumental delays in the signal to determine the cross-correlation as a function of τ, as described in Sect. 8.8.3.

3.3.4 Response to the Incident Radiation

We use subscripts 1 and 2 to indicate the two antennas and receiving channels as in Fig. 3.6. The response of antenna 1 to the signal field $E(l, m)$ given by Eq. (3.24) is the voltage spectrum $\widehat{V}(\nu)$. We multiply this by $H(\nu)$ to obtain the signal at the output of the filter, and then take the Fourier transform to go from the frequency to the time domain. Thus

$$V_{c1}(t) = \int_{-\infty}^{\infty}\int_{-\infty}^{\infty}\int_{-\infty}^{\infty} E(l,m)\sqrt{A_1(l,m)}H_1(\nu)e^{j2\pi\nu t}\, dl\, dm\, d\nu\ . \tag{3.28}$$

A similar expression can be written for the signal $V_{c2}(t)$ from antenna 2, and the output of the correlator is obtained from Eq. (3.27). Note also that if the radiation were to have some degree of spatial coherence, we should integrate over (l, m) independently for each antenna (Swenson and Mathur 1968), but here we make

[4]The term *correlator* basically refers to a device that measures the complex cross-correlation function $r(\tau)$, as given in Eq. (3.27). It is also used to denote simpler systems in which the time delay τ is zero or where both signals are represented by real functions. Large systems that cross-correlate the signal pairs of multielement arrays may contain 10^7 or more correlator circuits to accommodate many antennas and many spectral channels. Complete systems of this type are also commonly referred to as correlators.

the usual assumption of incoherence. Thus, the correlator output is

$$r(\tau) = \lim_{T\to\infty} \frac{1}{2T} \int_{-\infty}^{\infty}\int_{-\infty}^{\infty}\int_{-\infty}^{\infty}\int_{-\infty}^{\infty} E(l,m)E^*(l,m)\sqrt{A_1(l,m)A_2(l,m)}$$
$$\times\, H_1(\nu)H_2^*(\nu)e^{j2\pi\nu t}\, e^{-j2\pi\nu(t-\tau)}\, dl\, dm\, dt\, d\nu$$
$$= \int_{-\infty}^{\infty}\int_{-\infty}^{\infty}\int_{-\infty}^{\infty} I(l,m)\sqrt{A_1(l,m)A_2(l,m)}H_1(\nu)H_2^*(\nu)\, e^{j2\pi\nu\tau}\, dl\, dm\, d\nu\ . \tag{3.29}$$

Here, we have replaced the squared field amplitude by the intensity I. The result is a very general one since the use of separate response functions A_1 and A_2 for the two antennas can accommodate different antenna designs, or different pointing offset errors, or both. Also, different frequency responses H_1 and H_2 are used. In the case in which the antennas and filters are identical, Eq. (3.29) becomes

$$r(\tau) = \int_{-\infty}^{\infty}\int_{-\infty}^{\infty}\int_{-\infty}^{\infty} I(l,m)A(l,m)|H(\nu)|^2 e^{j2\pi\nu\tau}\, dl\, dm\, d\nu\ . \tag{3.30}$$

The result is a function of the delay τ of the signal $V_{c2}(t)$ with respect to $V_{c1}(t)$. The geometric component of the delay is generally compensated by an adjustable instrumental delay (discussed in Chaps. 6 and 7), so that $\tau = 0$ for radiation from the direction of the (l, m) origin. For a wavefront incident from the direction (l, m), the difference in propagation times through the two antennas to the correlator results from a difference in path lengths of $(ul + vm)$ wavelengths, for the conditions indicated in Eqs. (3.8) and (3.9). The corresponding time difference is $(ul + vm)/\nu$. If we take as V_1 the signal from the antenna for which the path length is the greater (for positive l and m), then from Eq. (3.30), the correlator output becomes

$$r = \int_{-\infty}^{\infty}\int_{-\infty}^{\infty}\int_{-\infty}^{\infty} I(l,m)A(l,m)|H(\nu)|^2 e^{-j2\pi(lu+mv)} dl\, dm\, d\nu\ . \tag{3.31}$$

Equation (3.31) indicates that the correlator output measures the Fourier transform of the intensity distribution modified by the antenna pattern. Let us assume that, as is often the case, the intensity and the antenna pattern are constant over the bandpass range of the filters, and the width of the source is small compared with the antenna beam. The correlator output then becomes

$$r = \int_{-\infty}^{\infty}\int_{-\infty}^{\infty} I(l,m)A(l,m)e^{-j2\pi(lu+mv)} dl\, dm \int_{-\infty}^{\infty} |H(\nu)|^2 d\nu$$
$$= A_0\mathcal{V}(u,v)\int_{-\infty}^{\infty} |H(\nu)|^2 d\nu\ , \tag{3.32}$$

where A_0 is the collecting area of the antennas in the direction of the maximum beam response and $\mathcal{V}$ is the visibility as in Eq. (3.2). The filter response $H(\nu)$ is a dimensionless (gain) quantity. If the filter response is essentially constant over a bandwidth $\Delta\nu$, Eq. (3.32) becomes

$$r = A_0 \mathcal{V}(u, v) \Delta\nu \ . \tag{3.33}$$

$\mathcal{V}(u, v)$ has units of W m^{-2} Hz^{-1}, A_0 has units of m^2, and $\Delta\nu$ has units of Hz. This is consistent with r, the output of the correlator, which is proportional to the correlated component of the received power.

Appendix 3.1 Mathematical Representation of Noiselike Signals

Electromagnetic fields and voltage waveforms that result from the emissions of astronomical objects are generally characterized by variations of a random nature. The received waveforms are usually described as ergodic (time averages and ensemble averages converge to equal values), which implies strict stationarity. For a detailed discussion, see, for example, Goodman (1985). Although such fields and voltages are entirely real, it is often convenient to represent them mathematically as complex functions. These complex functions can be manipulated in exponential form, and it is then necessary to take the real part as a final step in a calculation.

A3.1.1 Analytic Signal

A formulation that is often used in optical and radio signal analysis to represent a function of time is known as the *analytic signal*, which was introduced by Gabor (1946): see, for example, Born and Wolf (1999), Bracewell (2000), or Goodman (1985). Let $V_R(t)$ represent a real function of which the Fourier (voltage) spectrum is

$$\widehat{V}(\nu) = \int_{-\infty}^{\infty} V_R(t)\, e^{-j2\pi\nu t} dt \ . \tag{A3.1}$$

The inverse transform is

$$V_R(t) = \int_{-\infty}^{\infty} \widehat{V}(\nu)\, e^{j2\pi\nu t} d\nu \ . \tag{A3.2}$$

To form the analytic signal, the imaginary part that is added to produce a complex function is the Hilbert transform [see, e.g., Bracewell (2000)] of $V_R(t)$. One way of forming the Hilbert transform is to multiply the Fourier spectrum of the original

function by $j\,\mathrm{sgn}(\nu)$.[5] In forming the Hilbert transform of a function, the amplitudes of the Fourier spectral components are unchanged, but the phases are shifted by $\pi/2$, with the sign of the shift reversed for negative and positive frequencies. The Hilbert transform of $V_R(t)$, which becomes the imaginary part $V_I(t)$, is obtained as the inverse Fourier transform of the modified spectrum, as follows:

$$\begin{aligned} V_I(t) &= -j\int_{-\infty}^{\infty} \mathrm{sgn}(\nu)\widehat{V}(\nu)\, e^{j2\pi\nu t} d\nu \\ &= j\int_{-\infty}^{0} \widehat{V}(\nu)\, e^{j2\pi\nu t} d\nu - j\int_{0}^{\infty} \widehat{V}(\nu)\, e^{j2\pi\nu t} d\nu\ . \end{aligned} \tag{A3.3}$$

The analytic signal is the complex function that represents $V_R(t)$, and is

$$\begin{aligned} V(t) &= V_R(t) + jV_I(t) \\ &= \int_{-\infty}^{0} (1+j^2)\widehat{V}(\nu)\, e^{j2\pi\nu t} d\nu + \int_{0}^{\infty} (1-j^2)\widehat{V}(\nu)\, e^{j2\pi\nu t} d\nu \\ &= 2\int_{0}^{\infty} \widehat{V}(\nu)\, e^{j2\pi\nu t} d\nu\ . \end{aligned} \tag{A3.4}$$

It can be seen that the analytic signal contains no negative-frequency components. From Eq. (A3.4), another way of obtaining the analytic signal for a real function $V_R(t)$ is to suppress the negative-frequency components of the spectrum and double the amplitudes of the positive ones. It can also be shown [see, e.g., Born and Wolf (1999)] that

$$\langle [V_R(t)]^2 \rangle = \langle [V_I(t)]^2 \rangle = \tfrac{1}{2}\langle V(t)V^*(t) \rangle\ , \tag{A3.5}$$

where angle brackets $\langle\ \rangle$ indicate the expectation. The analytic signal is so called because, considered as a function of a complex variable, it is analytic in the lower half of the complex plane.

From Eqs. (A3.2) and (A3.4), we obtain

$$\int_{-\infty}^{\infty} \widehat{V}(\nu)\, e^{j2\pi\nu t} dt = 2\,\mathcal{R}e\left[\int_{0}^{\infty} \widehat{V}(\nu)\, e^{j2\pi\nu t} dt\right]\ . \tag{A3.6}$$

This is a useful equality that can be used with any *Hermitian*[6] function and its conjugate variable.

[5] The function $\mathrm{sgn}(\nu)$ is equal to 1 for $\nu \geq 0$ and -1 for $\nu < 0$. The Fourier transform of $\mathrm{sgn}(\nu)$ is $-j/\pi t$ (see Appendix 2.1).

[6] A Hermitian function is one in which the real part of the Fourier transform is an even function and the imaginary part is an odd function.

In many cases of interest in radio astronomy and optics, the bandwidth of a signal is small compared with the mean frequency ν_0, which in many instrumental situations is the center frequency of a filter. Such a waveform resembles a sinusoid with amplitude and phase that vary with time on a scale that is slow compared with the period $1/\nu_0$. The analytic signal can then be written as

$$V(t) = C(t)\, e^{j[2\pi\nu_0 t - \Phi(t)]} , \tag{A3.7}$$

where C and Φ are real. The spectral components of the function under consideration are appreciable only for small values of $|\nu - \nu_0|$. Thus, $C(t)$ and $\Phi(t)$ consist of low-frequency components, and the period of the time variation of C and Φ is characteristically the reciprocal of the bandwidth. The real and imaginary parts of the analytic signal can be written as

$$V_R(t) = C(t)\cos[2\pi\nu_0 t - \Phi(t)] , \tag{A3.8}$$

$$V_I(t) = C(t)\sin[2\pi\nu_0 t - \Phi(t)] . \tag{A3.9}$$

The modulus $C(t)$ of the complex analytic signal can be regarded as a modulation envelope, and $\Phi(t)$ represents the phase. In cases where the width of the signal band and the effect of the modulation are not important, it is clearly possible to consider C and Φ as constants, that is, to represent the signals as monochromatic waveforms of frequency ν_0, as in the introductory discussion. The case in which the bandwidth is small compared with the center frequency, as represented by Eq. (A3.7), is referred to as the quasi-monochromatic case.

As a simple example, $e^{j2\pi\nu t}$ is the analytic signal corresponding to the real function of time $\cos(2\pi\nu t)$. The Fourier spectrum of $e^{j2\pi\nu t}$ has a component at frequency ν only, but the Fourier spectrum of $\cos(2\pi\nu t)$ has components at the two frequencies $\pm\nu$. In general, it is necessary to consider the negative-frequency components in the analysis of waveforms, unless they are represented by the analytic signal formulation, for which negative-frequency components are zero. For example, in Eq. (2.8), we included negative-frequency components. If we had omitted the negative frequencies and doubled the amplitude of the positive ones, the cosine term in Eq. (2.9) would have been replaced by $e^{j2\pi\nu_0\tau}$. We would then have taken the real part to arrive at the correct result. In the approach used in Chap. 2, it is necessary to include the negative frequencies since the autocorrelation function is purely real, and thus its Fourier transform is Hermitian. In this book, we have generally included the negative frequencies rather than using the analytic signal and have made use of the relationship in Eq. (A3.6) when it is advantageous to do so.

It is interesting to note another property of functions of which the real and imaginary parts are a Hilbert transform pair. If the real and imaginary parts of a waveform (i.e., a function of time) are a Hilbert transform pair, then its spectral components are zero for negative frequencies. If we consider the inverse Fourier transforms, it is seen that if the waveform amplitude is zero for $t < 0$, the real and imaginary parts of the spectrum are a Hilbert transform pair. The response of any

electrical system to an impulse function applied at time $t = 0$ is zero for $t < 0$, since an effect cannot precede its cause. A function representing such a response is referred to as a *causal function*, and the Hilbert transform relationship applies to its spectrum.

A3.1.2 Truncated Function

Another consideration in the representation of waveforms concerns the existence of the Fourier transform. A condition of the existence of the transform is that the Fourier integral over the range $\pm\infty$ be finite. Although this is not always the case, it is possible to form a function for which the Fourier transform exists and that approaches the original function as the value of some parameter tends toward a limit. For example, the original function can be multiplied by a Gaussian so that the product falls to zero at large values, and the Fourier integral exists. The Fourier transform of the product approaches that of the original function as the width of the Gaussian tends to infinity. Such transforms in the limit are applicable to periodic functions such as $\cos(2\pi\nu t)$, as shown by Bracewell (2000). In the case of noiselike waveforms, the frequency spectrum of a time function can always be determined with satisfactory accuracy by analyzing a sufficiently long (but finite) time interval. In practice, the time interval needs to be long compared with the physically significant timescales that are associated with the waveform, such as the reciprocals of the mean frequency and of the bandwidth. Thus, if the function $V(t)$ is truncated at $\pm T$, the Fourier transform with respect to frequency becomes

$$\widehat{V}(\nu) = \lim_{T\to\infty} \frac{1}{2T} \int_{-T}^{T} V(t)\, e^{-j2\pi\nu t} dt \,. \tag{A3.10}$$

It is sometimes useful to define the truncated function as $V_T(t)$, where

$$\begin{aligned} V_T(t) &= V(t) \,, & |t| &\le T \,, \\ V_T(t) &= 0 \,, & |t| &> T \,, \end{aligned} \tag{A3.11}$$

and to write the Fourier transform as

$$\widehat{V}(\nu) = \lim_{T\to\infty} \frac{1}{2T} \int_{-\infty}^{\infty} V_T(t)\, e^{-j2\pi\nu t} dt \,. \tag{A3.12}$$

In the case of the analytic signal, truncation of the real part does not necessarily result in truncation of its Hilbert transform. It may therefore be necessary that the limits of the integral over time be $\pm\infty$, as in Eq. (A3.12), rather than $\pm T$.

References

Apostol, T.M., *Calculus*, Vol. II, Blaisdel, Waltham, MA (1962), p. 82

Born, M., and Wolf, E., *Principles of Optics*, 7th ed., Cambridge Univ. Press, Cambridge, UK (1999)

Bracewell, R.N., Radio Interferometry of Discrete Sources, *Proc. IRE*, **46**, 97–105 (1958)

Bracewell, R.N., *The Fourier Transform and Its Applications*, McGraw-Hill, New York (2000) (earlier eds. 1965, 1978)

Brouw, W.N., "Data Processing for the Westerbork Synthesis Radio Telescope," Ph.D. thesis, Univ. of Leiden (1971)

Gabor, D., Theory of Communication, *J. Inst. Elect. Eng.*, **93**, Part III, 429–457 (1946)

Goodman, J.W., *Statistical Optics*, Wiley, New York (1985)

König, A., Astrometry with Astrographs, in *Astronomical Techniques, Stars, and Stellar Systems*, Vol. 2, Hiltner, W.A., Ed., Univ. Chicago Press, Chicago (1962), pp. 461–486

Swenson, G.W., Jr., and Mathur, N.C., The Interferometer in Radio Astronomy, *Proc. IEEE*, **56**, 2114–2130 (1968)